

# A scan of $f(R)$ models admitting Rindler-type acceleration

S. Habib Mazharimousavi<sup>a</sup>, M. Kerachian<sup>b</sup>, M. Halilsoy<sup>c</sup>

Department of Physics, Eastern Mediterranean University, G. Magusa, North Cyprus, Mersin 10, Turkey

Received: 18 September 2013 / Accepted: 21 February 2014 / Published online: 15 March 2014  
© The Author(s) 2014. This article is published with open access at Springerlink.com

**Abstract** As a manifestation of a large distance effect Grumiller modified Schwarzschild metric with an extraneous term reminiscent of Rindler acceleration. Such a term has the potential to explain the observed flat rotation curves in general relativity. The same idea has been extended herein to the larger arena of  $f(R)$  theory. With particular emphasis on weak energy conditions (WECs) for a fluid we present various classes of  $f(R)$  theories admitting a Rindler-type acceleration in the metric.

## 1 Introduction

Flat rotation curves around galaxies constitute one of the most stunning astrophysical findings since 1930s. The cases can simply be attributed to the unobservable dark matter which still lacks a satisfactory candidate. On the general relativity side which reigns in the large universe an interesting approach is to develop appropriate models of constant centrifugal force. One such attempt was formulated by Grumiller in [1,2], in which the centrifugal force was given by  $F = -\left(\frac{m}{r^2} + a\right)$ . Here  $m$  represents the mass (both normal and dark), while the parameter “ $a$ ” is a positive constant—called Rindler acceleration [3]—which gives rise to a constant attractive force. The Newtonian potential involved is  $\Phi(r) \sim -\frac{m}{r} + ar$ , so that for  $r \rightarrow \infty$  the term  $\Phi(r) \sim ar$  becomes dominant. Since in Newtonian circular motion  $F = \frac{mv^2}{r}$ , for a mass  $m$ , tangential speed  $v(r)$  and radius  $r$  are related by  $v(r) \sim r^{\frac{1}{2}}$  for large  $r$ , which overall amounts to come slightly closer to the concept of flat rotation curves. No doubt, the details and exact flat rotation curves must be much more complicated than the toy model depicted here. Physically the parameter “ $a$ ” becomes mean-

ingful when one refers to an accelerated frame in a flat space, known as Rindler frame, and accordingly the terminology Rindler acceleration is adopted.

In [4] the impact of a Rindler-type acceleration is studied on the Oort cloud, and in [5,6] the solar system constraints on Rindler acceleration are investigated, while in [7] bending of light in the model of gravity at large distances proposed by Grumiller [1,2] is considered.

Let us add also that to tackle the flat rotation curves, Modified Newtonian Dynamics (MOND) in space was proposed [8]. Identifying a physical source for the Rindler acceleration term in the spacetime metric has been a challenge in recent years. An anisotropic fluid field was considered originally by Grumiller [1,2], whereas nonlinear electromagnetism was proposed as an alternative source [8]. A fluid model with an energy-momentum tensor of the form  $T_{\mu}^{\nu} = \text{diag}[-\rho, p, q, q]$  was proposed recently in the popular  $f(R)$  gravity [9]. For a review of the latter we propose [10–12]. By a similar strategy we wish to employ the vast richness of  $f(R)$  gravity models to identify possible candidates that may admit a Rindler-type acceleration. Our approach in this study beside the Rindler acceleration is to elaborate on the energy conditions in  $f(R)$  gravity. Although violation of the energy conditions is not necessarily a problem (for instance, any quantum field theory violates all energy conditions), it is still interesting to investigate the non-violation of the energy conditions. Note that energy conditions within the context of dark matter in  $f(R)$  gravity have been considered by various authors [13,14]. This at least will filter the viable models that satisfy the energy conditions. In brief, for our choice of energy-momentum the weak energy conditions (WECs) can be stated as follows: (1) WEC1 says that the energy density  $\rho \geq 0$ . (2) WEC2 says that  $\rho + p \geq 0$ , and (3) WEC3 states that  $\rho + q \geq 0$ . Among the more stringent energy conditions, the strong energy conditions (SECs) amounts further to  $\rho + p + 2q \geq 0$ , which will not be our concern in this paper. However, some of our models satisfy SECs as well. Our technical method can be summarized as follows.

<sup>a</sup> e-mail: habib.mazhari@emu.edu.tr

<sup>b</sup> e-mail: morteza.kerachian@cc.emu.tr

<sup>c</sup> e-mail: mustafa.halilsoy@emu.edu.tr

Upon obtaining  $\rho$ ,  $p$ , and  $q$  as functions of  $r$  we shall search numerically for the geometrical regions in which the WECs are satisfied. (A detailed treatment of the energy condition in  $f(R)$  gravity was given by J. Santos et al. in [15].)

From the outset our strategy is to assume the validity of the Rindler modified Schwarzschild metric a priori and search for the types of  $f(R)$  models which are capable to yield such a metric. Overall we test ten different models of  $f(R)$  gravity models and observe that in most cases it is possible to tune the free parameters in rendering the WECs satisfied. In doing this we entirely rely on numerical plots and we admit that our list is not an exhaustive one in the  $f(R)$  arena.

The organization of the paper goes as follows. Section 2 introduces the formalism with derivation of density and pressure components. Section 3 presents 11 types of  $f(R)$  models relevant to the Mannheim metric. The paper ends with our conclusion in Sect. 4.

### 2 The formalism

Let us start with the following action ( $\kappa = 8\pi G = 1$ ):

$$S = \frac{1}{2} \int \sqrt{-g} f(R) d^4x + S_M \tag{1}$$

where  $f(R)$  is a function of the Ricci scalar  $R$  and  $S_M$  is the physical source for a perfect fluid-type energy momentum,

$$T_{\mu}^{\nu} = \begin{pmatrix} -\rho & 0 & 0 & 0 \\ 0 & p & 0 & 0 \\ 0 & 0 & q & 0 \\ 0 & 0 & 0 & q \end{pmatrix} \tag{2}$$

We adopt the static spherically symmetric line element

$$ds^2 = -A(r) dt^2 + \frac{1}{A(r)} dr^2 + r^2 (d\theta^2 + \sin^2\theta d\varphi^2) \tag{3}$$

with

$$A(r) = 1 - \frac{2m}{r} + 2ar \tag{4}$$

which will be referred to henceforth as the Mannheim metric [16–18] (Note that it has been rediscovered by Grumiller in [1,2].) The Einstein field equations follow the variation of the action with respect to  $g_{\mu\nu}$ , reading

$$G_{\mu}^{\nu} = \frac{1}{F} T_{\mu}^{\nu} + \check{T}_{\mu}^{\nu}, \tag{5}$$

in which  $G_{\mu}^{\nu}$  is the Einstein tensor. The share of the curvature in the energy-momentum is given by

$$\check{T}_{\mu}^{\nu} = \frac{1}{F} \left[ \nabla^{\nu} \nabla_{\mu} F - \left( \square F - \frac{1}{2} f + \frac{1}{2} R F \right) \delta_{\mu}^{\nu} \right], \tag{6}$$

while  $T_{\mu}^{\nu}$  refers to the fluid source [1,2]. Following the standard notation,  $\square = \nabla^{\mu} \nabla_{\mu} = \frac{1}{\sqrt{-g}} \partial_{\mu} (\sqrt{-g} \partial^{\mu})$  and

$\nabla^{\nu} \nabla_{\mu} u = g^{\lambda\nu} \nabla_{\lambda} u_{,\mu} = g^{\lambda\nu} (\partial_{\lambda} u_{,\mu} - \Gamma_{\lambda\mu}^{\beta} u_{,\beta})$  for a scalar function  $u$ . The three independent Einstein field equations are explicitly given by

$$F R_t^t - \frac{f}{2} + \square F = \nabla^t \nabla_t F + T_t^t, \tag{7}$$

$$F R_r^r - \frac{f}{2} + \square F = \nabla^r \nabla_r F + T_r^r, \tag{8}$$

$$F R_{\theta_i}^{\theta_i} - \frac{f}{2} + \square F = \nabla^{\theta_i} \nabla_{\theta_i} F + T_{\theta_i}^{\theta_i}, \tag{9}$$

$$\left( F = \frac{df}{dR} \right), \tag{10}$$

in which  $\theta_i = (\theta, \varphi)$ . Adding these equations (i.e.,  $tt, rr, \theta\theta$  and  $\varphi\varphi$ ), one gets the trace equation

$$FR - 2f + 3\square F = T, \tag{11}$$

which is not an independent equation. Using the field equations one finds

$$\rho = \nabla^t \nabla_t F - F R_t^t + \frac{f}{2} - \square F, \tag{12}$$

$$p = -\nabla^r \nabla_r F + F R_r^r - \frac{f}{2} + \square F, \tag{13}$$

and

$$q = -\nabla^{\theta} \nabla_{\theta} F + F R_{\theta}^{\theta} - \frac{f}{2} + \square F. \tag{14}$$

In what follows we find the energy-momentum components for different models of  $f(R)$  gravity together with their thermodynamical properties.

### 3 $f(R)$ Models covering the Rindler acceleration

In this section we investigate a set of possible  $f(R)$  gravity models which admit the line element (3) as the static spherically symmetric solution of its field equations. Then by employing Eqs. (12–14) we shall find the energy density  $\rho$  and the pressures  $p$  and  $q$ . Having found  $\rho$ ,  $p$ , and  $q$  we investigate the energy conditions together with the feasibility of the  $f(R)$  models numerically. More precisely we work out the weak energy conditions, which includes the three individual conditions

$$WEC1 = \rho \geq 0, \tag{15}$$

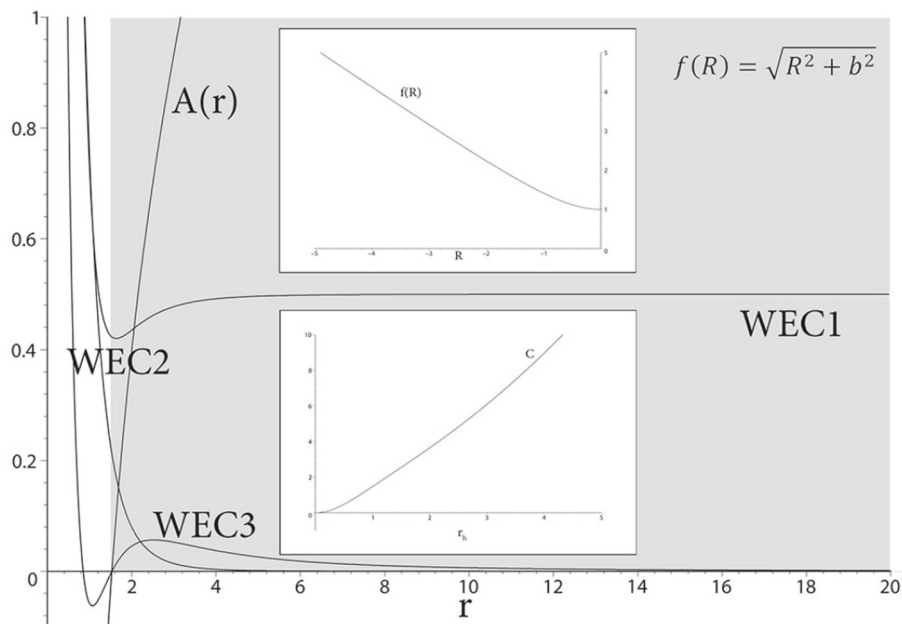
$$WEC2 = \rho + q \geq 0, \tag{16}$$

and

$$WEC3 = \rho + p \geq 0. \tag{17}$$

In the numerical plotting, we explicitly plot  $WEC1$ ,  $WEC2$ , and  $WEC3$  in terms of  $r$  to work out the region(s) in which the WECs are satisfied. In addition to the WECs we plot  $f(R)$  in terms of  $R$  to find the physically acceptable model

**Fig. 1** A plot of *WEC1*, *WEC2*, and *WEC3* for  $m = 1$ ,  $a = 0.1$ , and  $b = 1$ . To have an idea of the range in which the WECs are satisfied we also plot the metric function which identifies the location of the horizon. It is observed from the figure that the WECs are all satisfied for  $r \geq r_h$ , in which  $r_h$  is the event horizon of the Grumiller metric. Since  $R < 0$ , the plot of  $f(R)$  is from  $-\infty$  up to zero, and as can be seen we have  $\frac{df}{dR} < 0$ , while  $\frac{d^2f}{dR^2} > 0$ . We also plot the heat capacity  $C$  w.r.t. the horizon radius  $r_h$



by imposing the well-known conditions on  $f(R)$ , which are given by

$$F(R) = \frac{df(R)}{dR} > 0 \tag{18}$$

for not to have ghost field and

$$\frac{d^2f(R)}{dR^2} > 0 \tag{19}$$

to have a stable model. Before we start to study the  $f(R)$  models, we add that in the case of the Mannheim metric the Ricci scalar is given by  $R = -\frac{12a}{r}$ , which is negative ( $a > 0$ ).

### 3.1 The Models

1. Our first model which we find interesting is given by [19]

$$f(R) = \sqrt{R^2 + b^2} \tag{20}$$

for  $b = \text{constant}$ . For  $|R| \gg b$ , this model is a good approximation to Einstein's  $f(R) = R$  gravity. For the other range, namely  $|R| \ll b$ ,  $b$  may be considered as a cosmological constant. Taking this  $f(R)$  one finds

$$\frac{df}{dR} = \frac{R}{\sqrt{R^2 + b^2}}, \tag{21}$$

$$\frac{d^2f}{dR^2} = \frac{b^2}{(R^2 + b^2)^{3/2}}, \tag{22}$$

which are positive functions of  $R$ . This means that this model of  $f(R)$  gravity satisfies the necessary conditions to be physical. Yet we have to check the WECs at least to see whether it can be a good candidate for a spacetime with Rindler acceleration, namely the Mannheim metric. Figure 1 displays

*WEC1*, *WEC2*, and *WEC3* together with a part of  $A(r)$  in terms of  $r$ . We see that the WECs are satisfied right after the horizon. Therefore this model can be a good candidate for what we are looking for. This model is also interesting in other respects. For instance in the limit when  $b$  is small one may write

$$f(R) \simeq |R| + \frac{b^2}{2} \frac{|R|}{R^2}, \tag{23}$$

which is a kind of small fluctuation from  $R$  gravity for  $|R| \gg b$ .

In particular, this model of  $f(R)$  gravity is satisfying all necessary conditions to be a physical model to host the Mannheim metric. Hence we go one step further to check the heat capacity of the spacetime to investigate if the solution is stable from the thermodynamical point of view. To do so, first we find the Hawking temperature

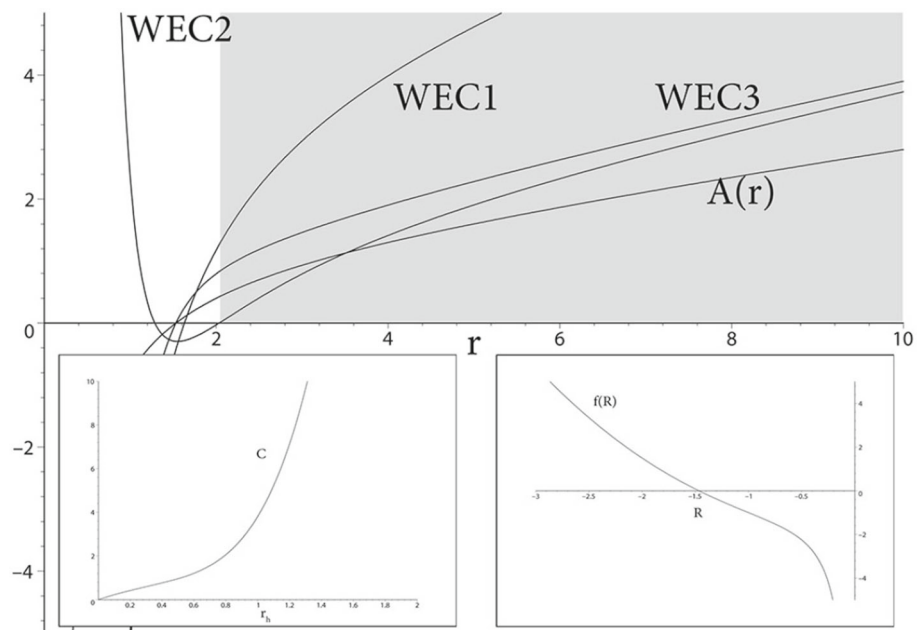
$$T_H = \left. \frac{\partial}{\partial r} g_{tt} \right|_{r=r_h} = \frac{m + ar_h^2}{2\pi r_h^2}. \tag{24}$$

Then from the general form of the entropy in  $f(R)$  gravity we find

$$S = \left. \frac{\mathcal{A}}{4G} F \right|_{r=r_h} = \pi r_h^2 F_h, \tag{25}$$

in which  $\mathcal{A}|_{r=r_h} = 4\pi r_h^2$  is the surface area of the black hole at the horizon and  $F|_{r=r_h} = \frac{-12a}{\sqrt{\frac{144a^2}{r_h^2} + b^2 r_h}}$ . Having  $T_H$  and  $S$  available one may find the heat capacity of the black hole as

**Fig. 2** Our choice of the parameters is  $\nu = 1, \mu = 2, b = 1, c = -1, \Lambda_1 = 0 = \Lambda_2$ . WECs are shown to be satisfied, while stability is valid only for  $R < -1$ . This can easily be checked from  $f(R) = R + \frac{1}{R} + R^2$ . Thermodynamic stability (i.e.  $C > 0$ ) is also shown



$$C = T \left( \frac{\partial S}{\partial T} \right) = \frac{12 (1 + 4ar_h) (288a^2 + b^2r_h^2) r_h^2 \pi a}{(144a^2 + b^2r_h^2)^{3/2}} \tag{26}$$

We comment here that  $C$  is always positive and nonsingular, irrespective of the values of the free parameters, given the fact that  $a > 0$ . This indeed means that the black hole solution will not undergo a phase change as expected from a stable physical solution.

2. The second model which we shall study, in this part, has been introduced and studied by Nojiri and Odintsov in [20]. As they have reported in their paper [20], “this model naturally unifies two expansion phases of the Universe: inflation at early times and cosmic acceleration at the current epoch”. This model of  $f(R)$  is given by

$$f(R) = R - \frac{c}{(R - \Lambda_1)^\nu} + b(R - \Lambda_2)^\mu, \tag{27}$$

in which  $b, c, \Lambda_1, \Lambda_2, \mu,$  and  $\nu$  are some adjustable parameters. Our plotting strategy of each model is such that if the WECs are violated (note that such cases are copious) we ignore such figures; the regions satisfying WECs are shaded. The other conditions  $\frac{df}{dR} > 0, \frac{d^2f}{dR^2} > 0$  are satisfied in some cases whereas in the other cases they are not. In Figs. 2 and 3 we plot WEC1, WEC2, and WEC3 in terms of  $r$  for specific values of  $\nu, \mu, b,$  and  $c$ , i.e., in Fig. 2  $\nu = 1, \mu = 2, b = 1, c = -1, \Lambda_1 = 0,$  and  $\Lambda_2 = 0$ . In Fig. 3  $\nu = 1, \mu = 3, b = -1, c = -1, \Lambda_1 = 0,$  and  $\Lambda_2 = 0$ .

Among the particular cases which are considered here, one observes that Fig. 2 and Fig. 3, which correspond to

$$f(R) = R + \frac{1}{R} + R^2 \tag{28}$$

and

$$f(R) = R + \frac{1}{R} - R^3, \tag{29}$$

respectively, are physically acceptable as far as WECs are concerned. We also note that in these two figures we plot the heat capacity in terms of  $r_h$  to show whether the solutions are thermodynamically stable.  $\frac{d^2f}{dR^2}$  reveals that Eqs. (28) and (29) are locally stable.

3. Our next model is a Born–Infeld-type version of gravity, which has been studied in the more general form of Dirac–Born–Infeld modified gravity by Quiros and Ureña-López in [21,22]. The Born–Infeld model of gravity is given by  $f(R) = 2b \left( 1 - \sqrt{1 + \frac{|R|}{b}} \right)$ , which implies

$$F(R) = \frac{1}{\sqrt{1 + \frac{|R|}{b}}} \tag{30}$$

and

$$\frac{d^2f}{dR^2} = \frac{1}{2 \left( 1 + \frac{|R|}{b} \right)^{3/2}}.$$

Clearly both are positive functions of  $R$ ; therefore the solution given in this model is stable and ghost-free. In spite of that, the WECs are not satisfied; therefore this model is not a proper model for the Mannheim metric as far as the energy conditions are concerned.

**Fig. 3** Our parameters in this case are  $\nu = 1, \mu = 2, b = -1, c = -1$ , with  $\Lambda_1 = 0 = \Lambda_2$ . Now  $f(R)$  takes the form  $f(R) = R + \frac{1}{R} - R^3$ , which satisfies the WECs. This choice yields a stable model for  $R < -\frac{1}{\sqrt[3]{3}}$ . Beyond a certain horizon radius the specific function  $C$  is also positive

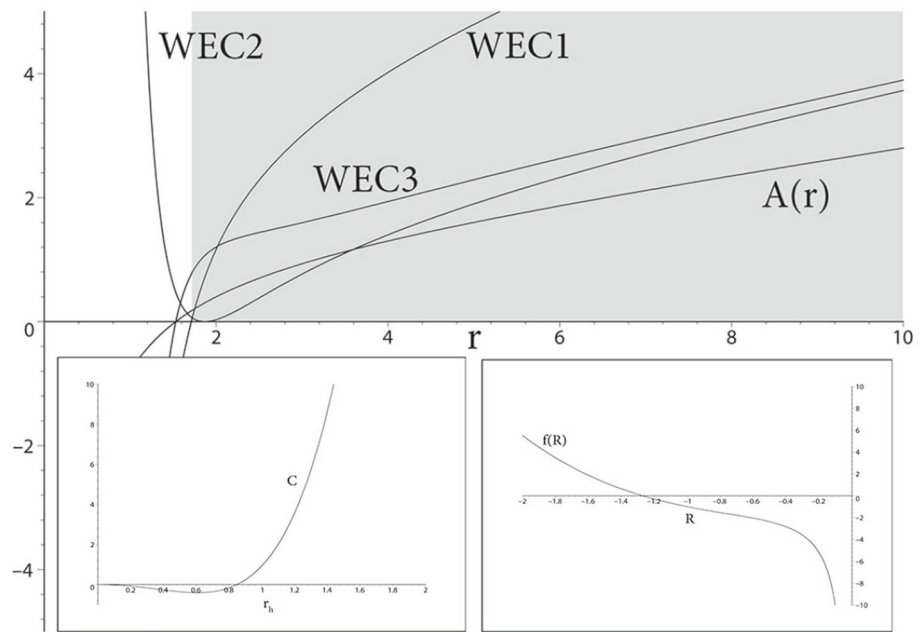
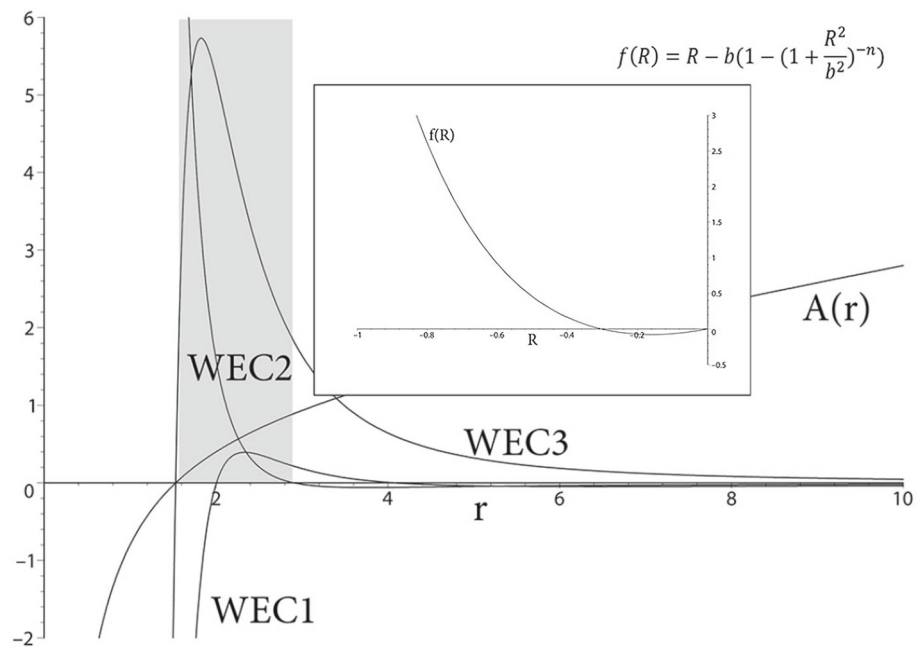


**Fig. 4** From Eq. (31) we choose the parameters as  $\mu = 1, b = 1$ , and  $n = -3$ . We find a restricted domain in which the WECs are satisfied. From those parameters beside WECs from  $\frac{d^2 f}{dR^2} = 6(1 + R^2)(1 + 5R^2) > 0$ , the stability condition also is satisfied



4. Another interesting model of  $f(R)$  gravity is given by [23]:

$$f(R) = R - \mu b \left[ 1 - \left( 1 + \frac{R^2}{b^2} \right)^{-n} \right], \tag{31}$$

in which  $\mu, b$ , and  $n$  are constants. Figure 4 with  $\mu = 1, b = 1, n = -3$  shows that between horizon and a maximum radius we may have a physical region in which  $f'' > 0$ . Now let us consider [24] the model

$$f(R) = R - \mu b \frac{\left(\frac{R}{b}\right)^{2n}}{\left(\frac{R}{b}\right)^{2n} + 1}, \tag{32}$$

which amounts to Fig. 5, and clearly there is no physical region.

5. Here, we use another model introduced in [25,26], which is given by

$$f(R) = R(1 - c) + c\varepsilon \ln \left( \frac{\cosh\left(\frac{R}{\varepsilon} - b\right)}{\cosh(b)} \right) + \frac{R^2}{6m^2}, \tag{33}$$

**Fig. 5** In this model given by the  $f(R)$  in Eq. (32) we have not been able to find a physically admissible region to satisfy the WECs

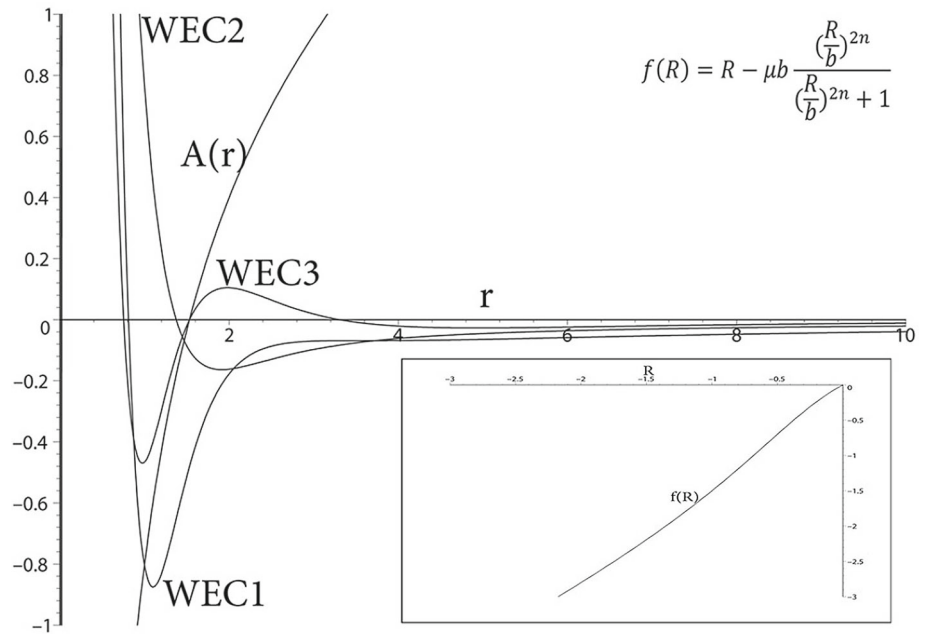
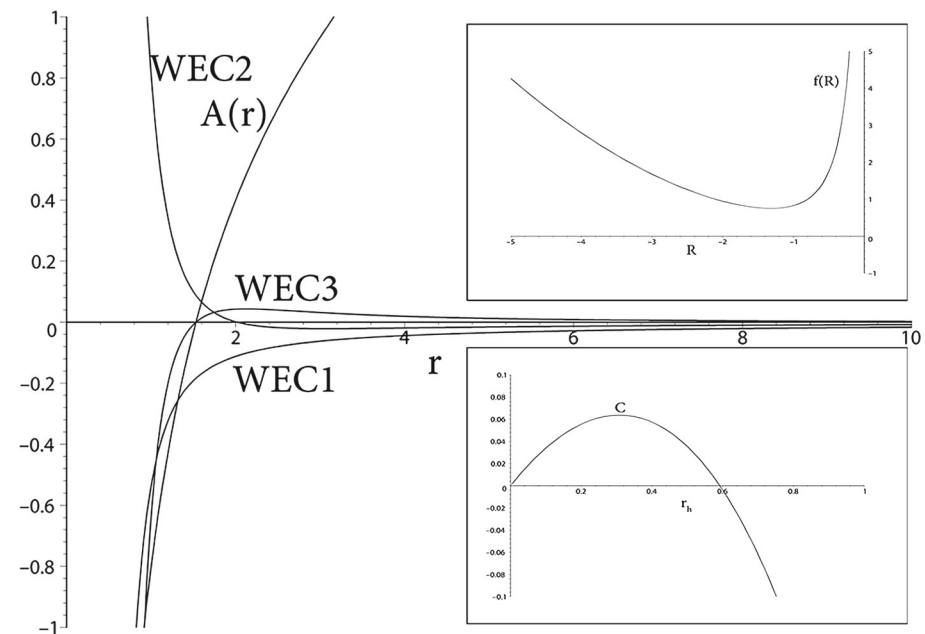


**Fig. 6** From the  $f(R)$  model in Eq. (33) the choice  $c = 1/3$ ,  $\varepsilon = 1$  and  $b = 1$ , we observe that WECs are not satisfied. The specific heat function is also pictured



in which  $c, \varepsilon, b,$  and  $\mu$  are all constants. Our analysis yields Fig. 6 with  $c = \frac{1}{3}$  and Fig. 7 with  $c = 1.1$ . One observes that although in Fig. 6 there is no physical region possible for different  $c$ , in Fig. 7 and for  $r > r_h$  our physical conditions are satisfied provided  $|R| < |R_0|$ , where  $R_0$  is the point for which  $f(R) = 0$ .

6. In Ref. [27] an exponential form of  $f(R)$  is introduced which is given by

$$f(R) = R e^{\frac{b}{R}}, \tag{34}$$

in which  $b = \text{constant}$  with first derivative

$$F(R) = e^{\frac{b}{R}} \left( 1 - \frac{b}{R} \right). \tag{35}$$

Our numerical plotting admits Fig. 8 for this model with  $b = -1$ . We comment here that although the case  $b = -1$  leads to the WECs being satisfied, in both cases  $f''(R)$  is negative. This makes the model unphysical.

7. Another exponential model, which is also given in [27], reads



**Fig. 7** The choice of parameters  $c = 1.1$ ,  $\varepsilon = 1$ , and  $b = 1$  in Eq. (33) yields a region where the WECs are satisfied. It can be checked that  $\frac{d^2 f}{dR^2} > 0$  is also satisfied. For  $|R| > |R_0|$ , where  $f'(R_0) = 0$ , we have  $\frac{df}{dR} > 0$ , which implies a ghost-free solution. The everywhere positive specific heat  $C$  is also shown

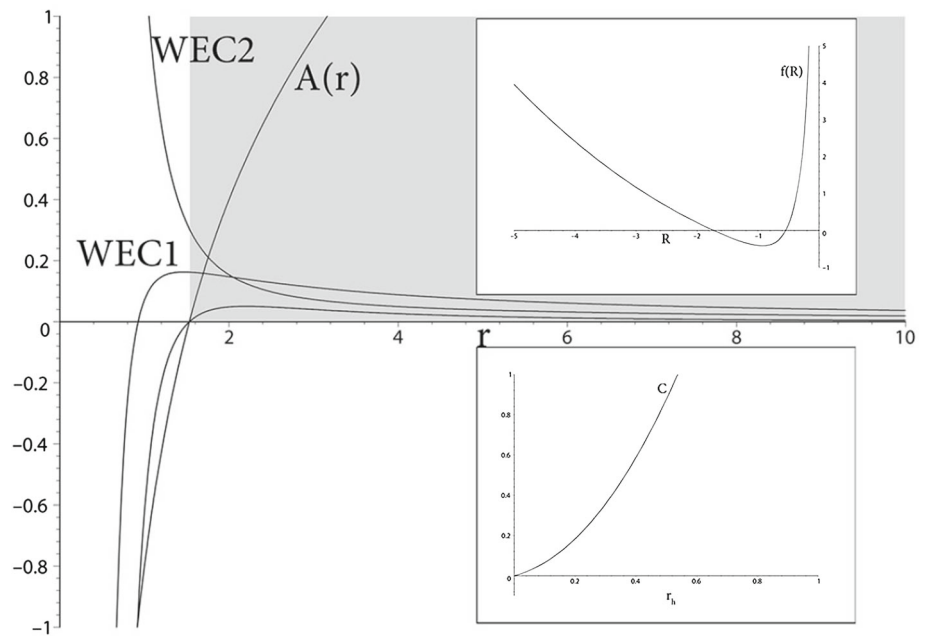
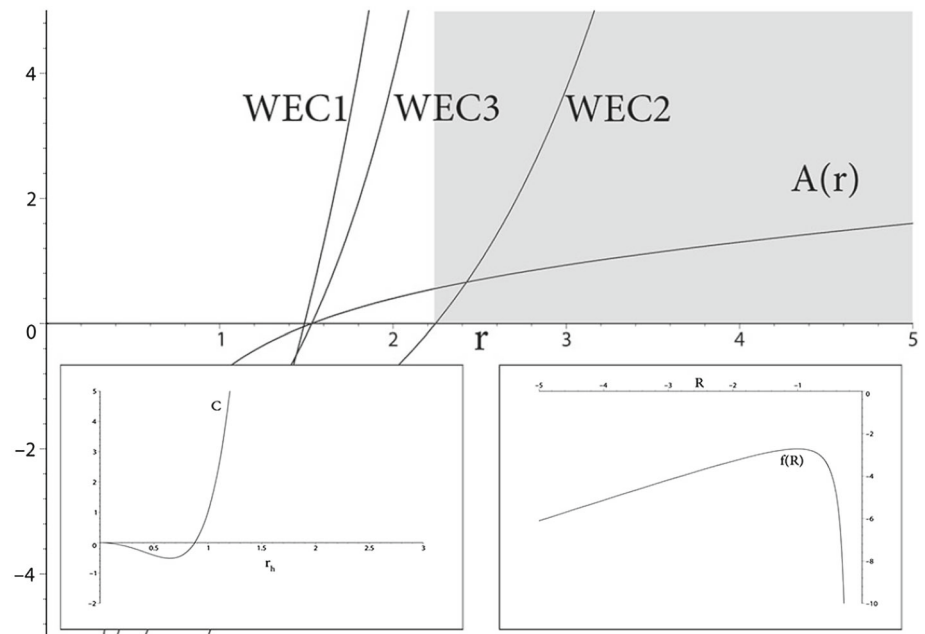


**Fig. 8** The model with  $f(R) = Re^{-\frac{1}{R}}$  gives a region in which WECs are satisfied. Furthermore, since  $\frac{d^2 f}{dR^2} = \frac{1}{R^3} e^{-\frac{1}{R}} < 0$ , it gives an unstable model. Beyond a certain radius the specific heat is also positive, which is required for thermodynamical stability



$$f(R) = Re^{bR}, \tag{36}$$

with  $b = \text{constant}$  and

in which  $b = \text{constant}$  and

$$F(R) = e^{bR} (1 + bR). \tag{37}$$

$$F(R) = e^{\frac{b}{R}} \left(1 - \frac{b}{R}\right) - 1.$$

This does not satisfy the energy conditions and therefore it is not a physically interesting case.

Figure 9 shows our numerical results with  $b = 0.1$ . For a region bounded from above and from below the WECs are satisfied, while  $f''(R)$  is negative, which makes our model unphysical.

8. In Ref. [28] a modified version of our models 6 and 7 is given in which

9. Among the exponential models of gravity let us consider [29,30]

$$f(R) = R \left( e^{\frac{b}{R}} - 1 \right),$$

$$f(R) = R + be^{\alpha R} \tag{38}$$

**Fig. 9** Our model in this case is given by  $f(R) = R \left( e^{\frac{b}{R}} - 1 \right)$  with  $b = \text{const}$ . With the choice  $b = 0.1$  it is observed that WECs are satisfied, while the stability condition is violated in spite of the fact that the specific heat  $C$  is everywhere positive

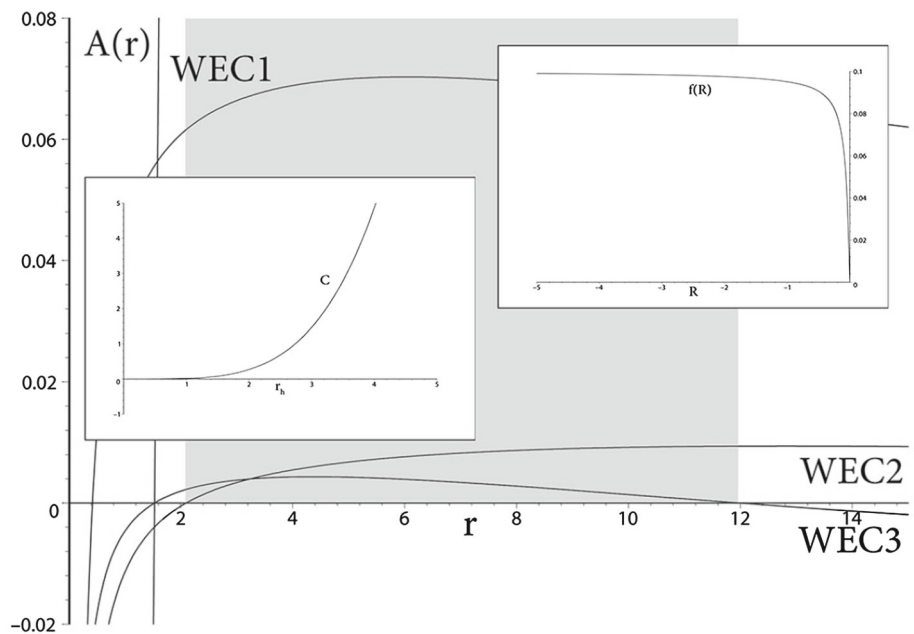
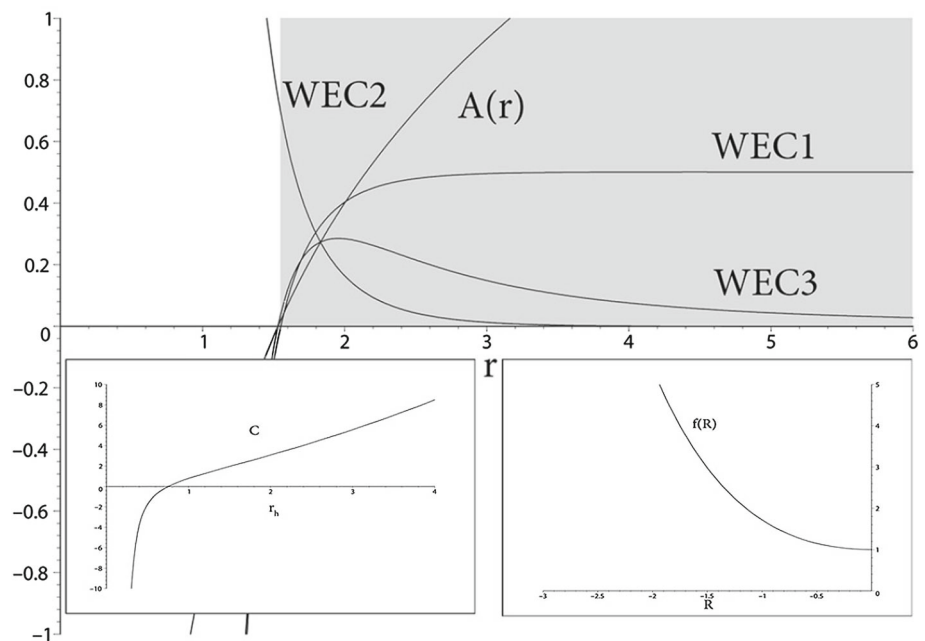


**Fig. 10** In this model we use  $f(R) = R + be^{\alpha R}$ , where  $\alpha$  and  $b$  are constants. For  $\alpha = -1$  and  $b = 1$ , the WECs are satisfied and  $\frac{d^2 f}{dR^2} > 0$ . The specific heat is shown also to be positive



where  $\alpha$  and  $b$  are constants and

$$F(R) = 1 + b\alpha e^{\alpha R}.$$

Figure 10 displays our numerical calculations for the specific value of  $\alpha = -1$ . Evidently from these figures we can conclude that this model is not a feasible model.

10. Finally we consider a model of gravity given in Ref. [31]

$$f(R) = \left( |R|^b - \Lambda \right)^{\frac{1}{b}}, \tag{39}$$

in which  $b$  is a constant. The first derivative of the model is given by

$$F(R) = |R|^{b-1} \left( |R|^b - \Lambda \right)^{\frac{1}{b}-1}.$$

Figures 11 and 12 are for  $b = \frac{1}{2}$  and  $b = 2$ , respectively, for  $\Lambda = 1$ . We observe that WECs are satisfied in a restricted region, while for  $b = 2 / \frac{1}{2}$  it gives a stable / unstable model.



**Fig. 11** Our model is given by  $f(R) = (|R|^2 - 1)^2$ , which has the WECs satisfied, but  $\frac{d^2f}{dR^2} > 0$ , for  $|R| > |R_0|$  where  $f'(R_0) = 0$ . This indicates the stability of the solution. Furthermore the specific heat suggests a thermodynamically stable model too

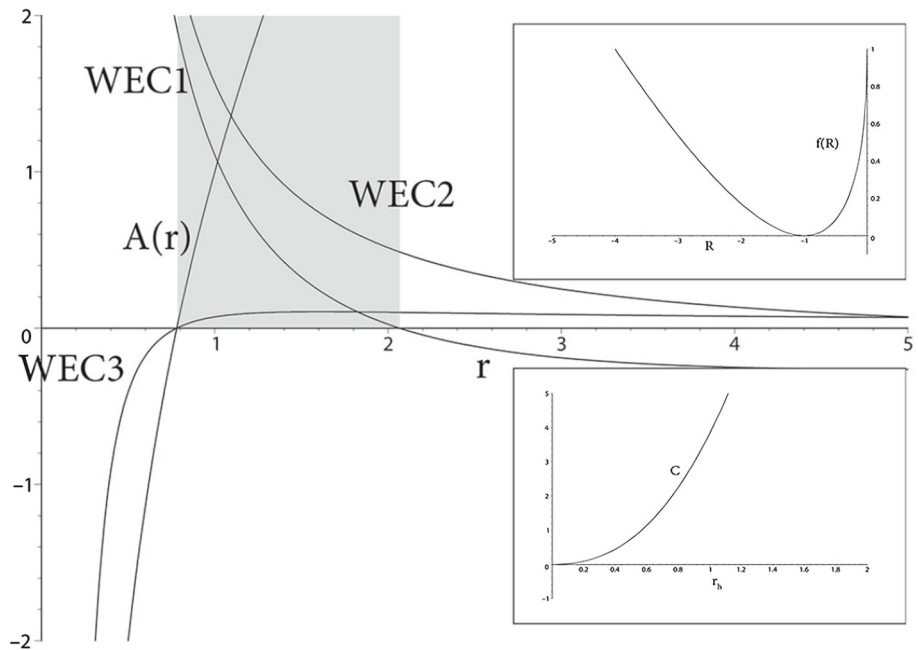
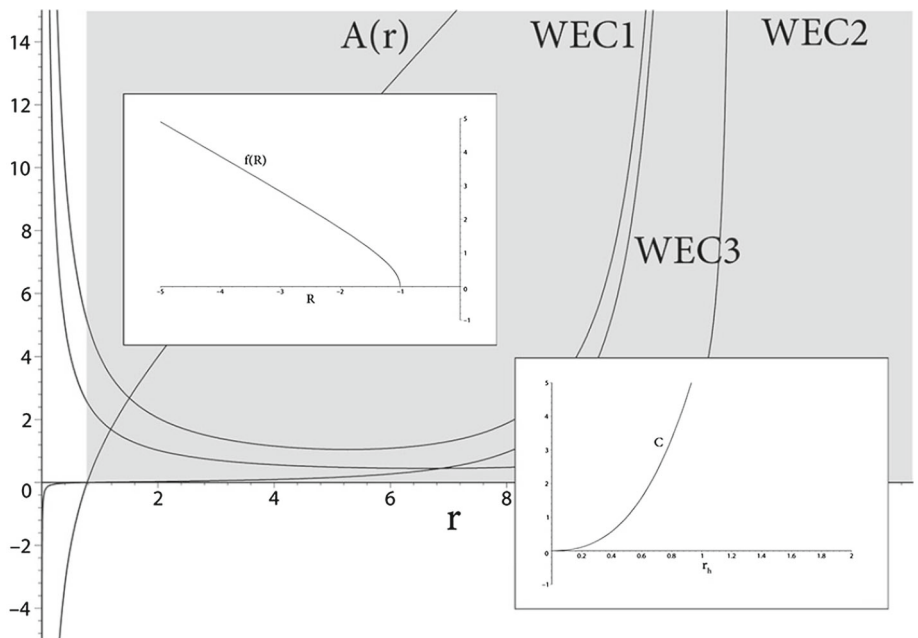


**Fig. 12** This is the model with  $f(R) = (|R|^{\frac{1}{2}} - 1)^{\frac{1}{2}}$ , which has the WECs all satisfied, while the stability condition is violated. It is thermodynamically stable since  $C > 0$



### 4 Conclusion

In Einstein's general relativity, which corresponds to  $f(R) = R$ , the Rindler modification of the Schwarzschild metric faces the problem that the energy conditions are violated. For a resolution to this problem we invoke the large class of  $f(R)$  theories. From a cosmological standpoint the main reason that we should insist on the Rindler acceleration term can be described as follows: at large distances such a term may explain the flat rotation curves as well as the dark matter problem. Our physical source beside the gravitational cur-

vature is taken to be a fluid with equal angular components. Being negative the radial pressure is repulsive in accordance with the expectations of the dark energy. Our scan covered ten different  $f(R)$  models and in most cases by tuning of the free parameters we show that the WECs are satisfied. In ten different models we searched primarily for the validity of WECs as well as for  $\frac{d^2f}{dR^2} > 0$ , i.e. the stability. With some effort thermodynamic stability can also be checked through the specific heat. With equal ease  $\frac{df}{dR} > 0$ , i.e., the absence of ghosts can be traced. Figure 1, for instance, depicts the model with  $f(R) = \sqrt{R^2 + b^2}$ , ( $b = \text{constant}$ ) in which WECs and

stability, even the thermodynamic stability, are all satisfied, however, it hosts ghosts since  $\frac{df}{dR} < 0$  for  $R < 0$ . Finally, among all models considered herein, we note that Fig. 7 satisfies WECs, stability conditions, as well as the ghost-free condition for  $r > r_{\min}$  in which  $r_{\min} \geq r_h$  depends on the other parameters.

Finally we comment that the abundance of parameters in the  $f(R)$  theories is one of its weak aspects. This weakness, however, may be used to obtain various limits and for this reason particular tuning of parameters is crucial. Our requirements have been weak energy conditions (WECs), Rindler acceleration, stability, and the absence of ghosts. Naturally further restrictions will add further constraints, which may lead us to dismiss some cases that are considered as viable in this study.

**Open Access** This article is distributed under the terms of the Creative Commons Attribution License which permits any use, distribution, and reproduction in any medium, provided the original author(s) and the source are credited.

Funded by SCOAP<sup>3</sup> / License Version CC BY 4.0.

## References

1. D. Grumiller, Phys. Rev. Lett. **105**, 211303 (2010), 039901(E) (2011)
2. S. Carloni, D. Grumiller, F. Preis, Phys. Rev. D **83**, 124024 (2011)
3. W. Rindler, *Essential Relativity: Special, General, and Cosmological*. 2nd edn. (Springer, Berlin, 1977)
4. L. Iorio, Mon. Not. R. Astron. Soc. **419**, 2226 (2012)
5. L. Iorio, JCAP **05**, 019 (2011)
6. J. Sultana, D. Kazanas, Phys. Rev. D **85**, 081502 (2012)
7. M. Milgrom, Astrophys. J. **270**, 365 (1983)
8. M. Halilsoy, O. Gurtug, S. H. Mazharimousavi, arXiv:1212.2159.
9. S.H. Mazharimousavi, M. Halilsoy, Mod. Phys. Lett. A **28**, 1350073 (2013)
10. S. Nojiri, S.D. Odintsov, Phys. Rep. **505**, 59 (2011)
11. A. De Felice, S. Tsujikawa, Living Rev. Rel. **13**, 3 (2010)
12. T.P. Sotiriou, V. Faraoni, Rev. Mod. Phys. **82**, 451 (2010)
13. S. Capozziello, V.F. Cardone, S. Carloni, A. Troisi, Phys. Lett. A **326**, 292 (2004)
14. C. Frigerio Martins, P. Salucci, Mon. Not. R. Astron. Soc. **381**, 1103 (2007)
15. J. Santos, J.S. Alcaniz, M.J. Rebouças, F.C. Carvalho, Phys. Rev. D **76**, 083513 (2007)
16. P. Mannheim, Prog. Part. Nucl. Phys. **56**, 340 (2006)
17. H. Culetu, Int. J. Mod. Phys. Conf. Ser. **3**, 455 (2011)
18. H. Culetu, Phys. Lett. A **376**, 2817 (2012)
19. M.S. Movahed, S. Baghram, S. Rahvar, Phys. Rev. D **76**, 044008 (2007)
20. S. Nojiri, S. Odintsov, Phys. Rev. D **68**, 123512 (2003)
21. D.N. Vollick, Phys. Rev. D **69**, 064030 (2004)
22. I. Quiros, L.A. Ureña-López, Phys. Rev. D **82**, 044002 (2010)
23. A.A. Starobinsky, J. Exp. Theor. Phys. Lett. **86**, 157 (2007)
24. W. Hu, I. Sawicki, Phys. Rev. D **76**, 064004 (2007)
25. S.A. Appleby, R.A. Battye, A.A. Starobinsky JCAP **06**, 005 (2010).
26. S.A. Appleby, R.A. Battye, JCAP **05**, 019 (2008).
27. L. Amendola, R. Gannouji, D. Polarski, S. Tsujikawa, Phys. Rev. D **75**, 083504 (2007)
28. Z. Girones, A. Marchetti, O. Mena, C. Pena-Garay, N. Rius, JCAP **11**, 004 (2010)
29. G. Cognola, E. Elizalde, S. Nojiri, S.D. Odintsov, L. Sebastiani, S. Zerbini, Phys. Rev. D **77**, 046009 (2008)
30. E. Elizalde, S. Nojiri, S.D. Odintsov, L. Sebastiani, S. Zerbini, Phys. Rev. D **83**, 086006 (2011)
31. L. Amendola, S. Tsujikawa, Phys. Lett. B **660**, 125 (2008)